

Introduction to System-on-Chip and its Applications

Individual Project Report

3D Sensing for Vehicle Technologies



Department: Institute of Comm. Engineering

Student ID: 110064533

Name: 陳劭珩 (Shao-Heng Chen)

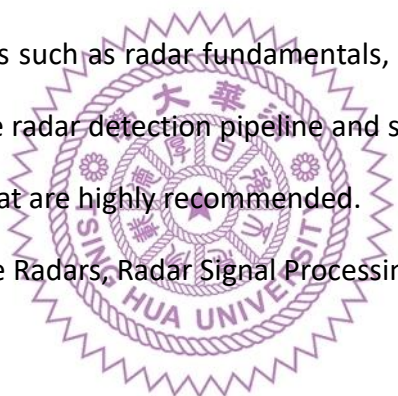
Instructor: 邱瀟德 教授 (Prof. Ching Te Chiu)

December 2022

Abstract

There have been significant improvements in the performance of automotive radar due to recent developments. The next generation of 4D radar is capable of generating high-resolution point clouds, providing imaging capability. This technology is poised to play a major role in the development of radar perception for autonomous driving systems. In this context, we believe that the era of using radar for Advanced driver assistance systems (ADAS) has arrived. However, most researchers are focusing on LiDAR and Vision algorithm, while studies on radar deep learning are spread across different tasks, and a holistic overview is lacking. This paper aims to provide a fundamental introduction to the deep radar perception stack for researchers who are new to this field. It covers topics such as radar fundamentals, signal processing, common modulation waveforms, the radar detection pipeline and some off-the-shelf radar micro control units (MCUs) that are highly recommended.

keywords: Automotive Radars, Radar Signal Processing, Radar Sensing.



Contents

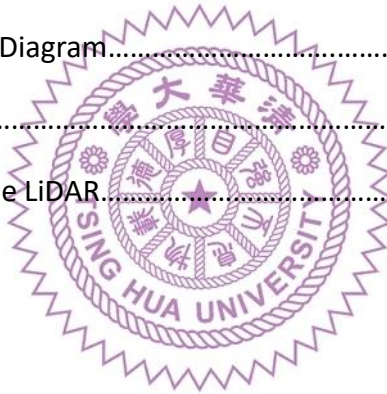
Abstract.....	i
List of Figures.....	iv
List of Tables.....	iv
Chapter 1 Introduction.....	1
1.1 Motivation.....	1
Chapter 2 Technology	4
2.1 Radar Signal Processing Fundamentals	4
2.1.1 FMCW Radar Signal Processing	4
2.1.2 FMCW Radar Performances	7
2.1.3 Common Modulation Waveforms	9
2.1.4 Radar Object Detection Pipeline	12
Chapter 3 Case Study – TI AWR 2944 EVM	13
3.1 TI AWR 2944 EVM Overview	13
3.2 TI AWR 2944 EVM Features	14
3.3 TI AWR 2944 Spec	14
3.3.1 TI AWR 2944 chip parameters	14
3.3.2 Block Diagram.....	15
Chapter 4 Applications and its opponents	16
4.1 Applications	16

4.2 Opponents.....	16
4.2.1 Vision - Comma ai Driver Assistance System.....	16
4.2.2 LiDAR - Velodyne HDL-64E LiDAR Sensor.....	18
Chapter 5 Conclusion	20
Reference	21



List of Figures

Figure 1. FMCW waveform.....	6
Figure 2. Sampling points matrix.....	7
Figure 3. 2D FFT Process.....	8
Figure 4. Unmodulated CW.....	10
Figure 5. Fast chirp FMCW.....	10
Figure 6. Slow chirp.....	11
Figure 7. FMCW Pulsed CW.....	11
Figure 8. FSK modulation.....	12
Figure 9. AWR2944EVM.....	14
Figure 10. Functional Block Diagram.....	16
Figure 11. Block Diagram.....	16
Figure 12. Velodyne's 64-line LiDAR.....	20



List of Tables

Table 1. Equations for radar performance.....	9
Table 2. Typical automotive radar parameters.....	9
Table 3. TI AWR2944 parameters.....	15
Table 4. Comma Three spec.....	18
Table 5. Velodyne's 64-line LiDAR spec.....	20
Table 6. SWOT analysis of Radar Sensors.....	21

Chapter 1 Introduction

1.1 Motivation

As autonomous driving technology advances from the demonstration phase to the implementation phase, it demands higher levels of perception capability. The most widely used autonomous driving systems rely on combining cameras and LiDARs for perception. While millimeter wave radar has been commonly utilized in mass-produced vehicles for active safety functions like automatic emergency braking (AEB) and forward collision warning (FCW), it has not been a popular choice for autonomous driving. [1]

Previously, Tesla announced that it would be removing radar sensors from its semi-autonomous driving system Autopilot. In June 2021, at the Computer Vision and Pattern Recognition (CVPR) workshop (held in 2021) [2], Tesla's Director of AI, Andrej Karpathy, explained the reasoning behind their decision by presenting three common scenarios where radar malfunctions occur, including the loss of tracking due to significant deceleration of the front vehicle, false slowdowns under bridges, and missed detection of a stationary vehicle parked on the side of the main road. The first issue is related to sidelobes and the close field detection ability of radar. Conventional radars with a limited number of channels are not effective at sidelobe compression. The second case occurs because conventional radar cannot measure height information, leading it to confuse overhead bridges with stationary objects on the road. The third case is due to the low angular resolution of conventional radar, which prevents it from accurately capturing the shape of a stationary vehicle. These challenges can be addressed with the use of next-generation high-resolution radar.

Recently, Tesla informed the Federal Communications Commission (FCC) that it intends to begin selling a new radar in mid-January 2022. In its request, the company confirmed its plans to start marketing the new device next month. In June of last year, Tesla CEO Elon Musk told Electrek, a news website that focuses on the electric vehicle (EV) industry and renewable energy, that the company stopped using radar in its vehicles: "the probability of safety will be higher with pure vision than vision plus radar, not lower. Vision has become so good that radar actually reduces signal/noise." However, he also mentioned that Tesla might consider using radar again in the future if it had access to a very high-resolution radar: "A very high-resolution radar would be better than pure vision, but such a radar does not exist. I mean vision with high-resolution radar would be better than pure vision." From recent news we saw some indications that Tesla is working on developing such a radar. [3]

Radar is often compared to LiDAR as a ranging sensor. A typical 77 GHz automotive radar has a wavelength of 3.9 mm, while automotive LiDARs have much smaller wavelengths of 905 nm or 1550 nm. For a radar with a small aperture, most of the reflected signal is not received by the sensor due to specular reflection. Another issue with a small aperture is the low angular resolution, which makes it difficult to distinguish between two close objects. These features result in a radar point cloud that is sparser than a LiDAR point cloud. Conventional automotive radars have low resolution in elevation and therefore only produce a two-dimensional point cloud. The next generation of high-resolution radar has higher angular resolution in both azimuth and elevation and can measure 3D position and Doppler velocity, making it referred to as a 4D radar in the market.

It can be seen that traditional long-range radars have low angular resolution in the horizontal view and no resolution in the vertical view. In contrast, 4D radar has an angular resolution of about 1° in both horizontal and vertical views, allowing it to accurately classify static objects. Radar can also measure Doppler velocity and radar cross-section, which can aid in classifying road users. In addition, 4D radar has a long detection range of up to 300 m, can operate in all weather conditions, has low power consumption, and is cost-effective. Therefore, we believe that radar is a valuable complement to LiDAR and vision, and the fusion of these sensors allows for all-weather, long-range environment perception.



Chapter 2 Technology

2.1 Radar Signal Processing Fundamentals

Knowledge of radar signal processing is essential for the development of a radar 3D sensing system. The sensing capabilities of different radar devices can vary. In order to effectively utilize radar technology, it is important to have a fundamental understanding of the performance limitations, identify key scenarios, and address critical issues. This section presents a classical signal processing pipeline commonly used in automotive radar applications.

2.1.1 FMCW Radar Signal Processing

Automotive radars that are readily available on the market use a series of linear frequency-modulated continuous-wave (FMCW) signals to measure range, angle, and velocity simultaneously. These radars are permitted to operate in two millimeter-wave bands according to regulations: 24 GHz (24–24.25 GHz) and 77 GHz (77–79 GHz). The 77 GHz band is becoming increasingly popular due to its wider bandwidth (76–77 GHz for long-range and 77–81 GHz for short-range), higher Doppler resolution, and smaller antenna with sub-wavelength size [4].

As shown in Figure 1, the FMCW signal is characterized by the start frequency (also known as the carrier frequency) f_c , the sweep bandwidth B , the chirp duration T_c , and the slope $S = B / T_c$. During one chirp duration, the frequency increases linearly from f_c to $f_c + B$ with a slope of S . One FMCW waveform is referred to as a chirp, and radar transmits a frame of N_c chirps equally spaced by chirp cycle time T_c . The

total time $T_f = N_c \cdot T_c$ is called the frame time, also known as the time on target (TOT).

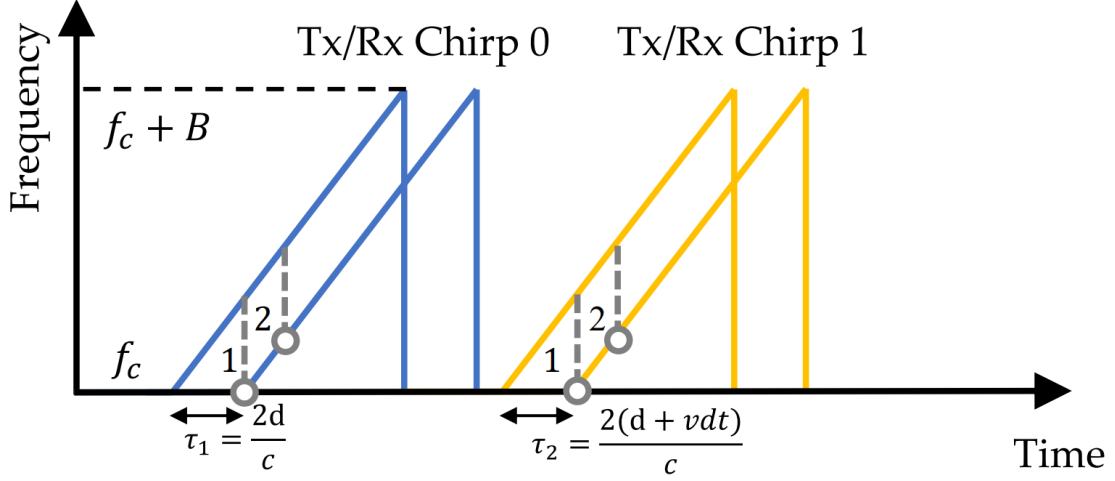


Figure 1. FMCW waveform

In order to avoid the need for high-speed sampling, a frequency mixer combines the received signal with the transmitted signal to produce two signals with sum frequency $f_T(t) + f_R(t)$ and difference frequency $f_T(t) - f_R(t)$. Then, a low-pass filter is used to filter out the sum frequency component and obtain the intermediate frequency (IF) signal. In this way, FMCW radar can achieve GHz performance with only MHz sampling. In practice, a quadrature mixer is used to improve the noise figure [5], resulting in a complex exponential IF signal as $X_{IF}(t) = Ae^{j(2\pi f_{IF}t + \phi_{IF})}$ where A is the amplitude, $f_{IF} = f_T(t) - f_R(t)$ is referred to as the beat frequency, and ϕ_{IF} is the phase of the IF signal. Next, the IF signal is sampled N_s times by an ADC converter, resulting in a discrete-time complex signal. Multiple frames of chirp signals are assembled into a two-dimensional matrix.

As shown in Figure 2, the dimension of the sampling points within a chirp is referred to as fast time, and the dimension of the chirp index within one frame is referred to as slow time. Assuming one object moving with speed v at distance r , the frequency

and phase of the IF signal are given by $f_{IF} = \frac{2S(r+vt_c)}{c}$ and $\phi_{IF} = \frac{4\pi(r+vt_c)}{\lambda}$ where $\lambda = c / f_c$ is the wavelength of the chirp signal. From the above two relations we can find that the range and Doppler velocity are coupled.

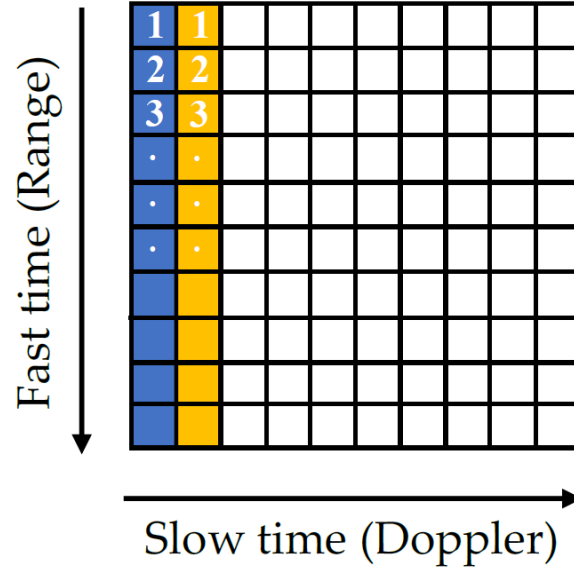


Figure 2. Sampling points matrix

Under the following assumptions: (1) the range variations in slow time caused by target motion can be neglected due to the short frame time; (2) the Doppler frequency in fast time can be neglected compared to the beat frequency by utilizing a wideband waveform. Then, range and Doppler can be decoupled. Range can be estimated from the beat frequency as $r = cf_{IF} / 2S$, and Doppler velocity can be estimated from the phase shift between two chirps as $v = \Delta\phi\lambda / 4\pi T_c$.

Next, a range FFT is applied in the fast-time dimension to resolve the frequency change, followed by a Doppler FFT in the slow-time dimension to resolve the phase change, and the process is shown in Figure 3. As a result, we obtain a 2D complex-valued data matrix called the Range–Doppler (RD) map. In practice, a window function is applied before DFT to reduce sidelobes. The range and the Doppler velocity of a cell

in the RD map are given by $r_k = kc / 2B_{IF}$ and $v_l = l\lambda / 2T_f$ where k and l denote the indexes of FFT, B_{IF} is the IF bandwidth, and T_f is the frame time. In practice, FFT is applied due to its computational efficiency. Accordingly, the sequence will be zero-padded to the nearest power of 2 if necessary. Angle information can be obtained using more than one receive or transmit channel.

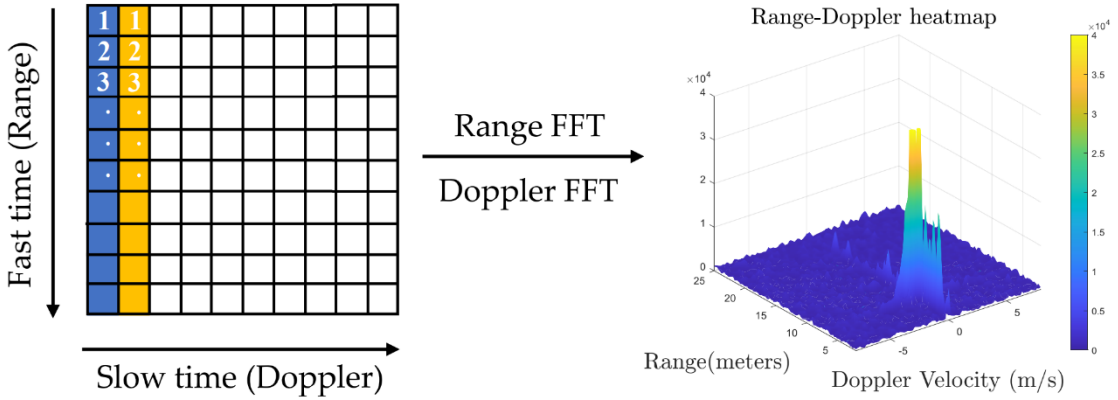


Figure 3. 2D FFT Process

2.1.2 FMCW Radar Performances

The performance of automotive radar can be evaluated in terms of maximum range, maximum Doppler velocity, and field of view (FoV). Equations for these attributes are summarized in Table 1. According to the radar equation, the theoretical maximum detection range is given by $R_{max} = \sqrt[4]{P_t G^2 \lambda^2 \sigma / (4\pi)^3 P_{min}}$ where P_t is the transmit power, P_{min} is the minimum detectable signal or receiver sensitivity, λ is the transmit wavelength, σ is the target RCS, and G is the antenna gain. The wavelength is 3.9 mm for automotive 77 GHz radar. The target RCS is a measure of the ability to reflect radar signals back to the radar receiver. It is a statistical quantity that varies with the viewing angle and the target material. Some typical values for these parameters are summarized in Table 2. In practice, the maximum range is limited by the supported

IF bandwidth B_{IF} and ADC sampling frequency. The maximum unambiguous velocity is inversely proportional to the chirp duration T_c .

Definition	Equation
Max Unambiguous Range	$R_m = \frac{c \cdot B_{IF}}{2S}$
Max Unambiguous Velocity	$v_m = \frac{\lambda}{4T_c}$
Max Unambiguous Angle	$\theta_{FoV} = \pm \arcsin\left(\frac{\lambda}{2d}\right)$
Range Resolution	$\Delta R = \frac{c}{2B}$
Velocity Resolution	$\Delta v = \frac{\lambda}{2N_c \cdot N_T}$
Angular Resolution	$\Delta \theta_{res} = \frac{\lambda}{N_R \cdot d \cdot \cos(\theta)}$
3 dB Beamwidth	$\Delta \theta_{3dB} = 2 \arcsin\left(\frac{1.4\lambda}{\pi \cdot D}\right)$

Table 1. Equations for radar performance

Parameter	Range
Transit power	10 ~ 13 (dBm)
TX / RX antenna gain	10 ~ 25 (dBi)
Receiver noise figure	10 ~ 20 (dB)
Target Radar Cross Section (RCS)	−10 ~ 20 (dBsm)
Receiver sensitivity	−120 ~ −115 (dBm)
Minimum SNR	10 ~ 20 (dB)

Table 2. Typical automotive radar parameters

2.1.3 Common Modulation Waveforms

According to the investigation results [7], there are five common modulation patterns: (a) Unmodulated CW, (b) Fast chirp FMCW (Sawtooth modulation), (c) Slow chirp FMCW (Triangular modulation), (d) Pulsed CW (Square-wave modulation), and (e) FSK (Stepped modulation), respectively.

(a) Unmodulated CW: This modulation pattern is used for some millimeter wave communication signals and the signal frequency will remain the same within a period of time, as shown in Figure 4. The transmitted signal is given by $s_{tcw}(t) = A_T \exp(j2\pi f_{cw}t)$, $0 \leq t < T$ where A_T is the transmitted signal strength, T is the transmission period, and f_{cw} is the carrier frequency.

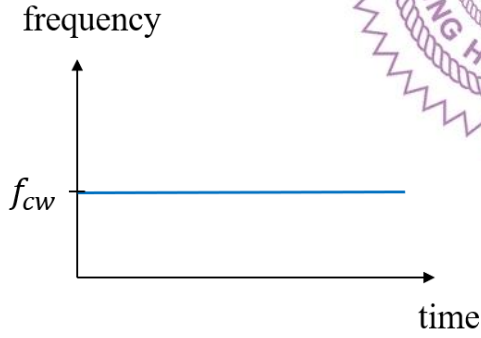


Figure 4. Unmodulated CW

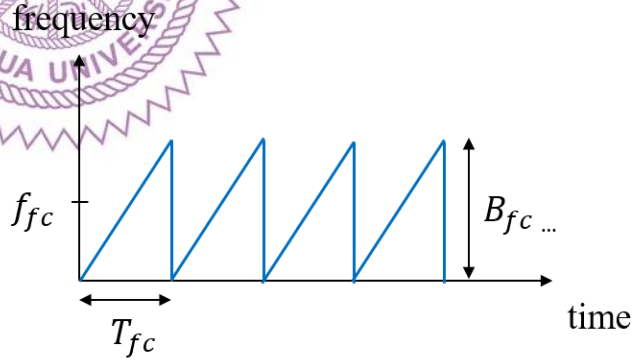


Figure 5. Fast chirp FMCW

(b) Fast chirp FMCW (a.k.a. Sawtooth modulation): This modulation pattern is used in a relatively large range (maximum distance) combined with a negligible influence of Doppler frequency, shown in Figure 5. The transmitted signal is given by $s_{tfc}(t) = A_T \exp\left(j2\pi\left(f_{fc}t + \frac{B_{fc}f_{fc}}{2T_{fc}}t^2\right)\right)$, $0 \leq t < T$ where f_{fc} , B_{fc} , and T_{fc} represent its carrier frequency, transmission bandwidth and the time period of single continuous wave

frequency. Most importantly, fast chirp FMCW actually accounts for 90% of the modulation we are likely to see in our daily lives.

(c) Slow chirp FMCW (a.k.a. Triangular modulation): This modulation pattern allows easy separation of the difference frequency Δf of the Doppler frequency f_D , shown in Figure 6. The transmitted signal is given by

$$s_{tsc}(t) = A_T \exp \left(j2\pi \left(\left(f_{sc} + (-1)^k B_{sc} \left(\frac{1}{2} + k \right) \right) t - (-1)^k \frac{B_{sc}}{2T_{sc}} t^2 \right) \right),$$

$0 \leq t < T$ where f_{sc} , B_{sc} , and T_{sc} represent its carrier frequency, transmission bandwidth and the time period of single continuous wave frequency. T_{sc} also indicates whether the signal is a up-chirp signal or a down-chirp signal, and k is the index of the modulated signal.

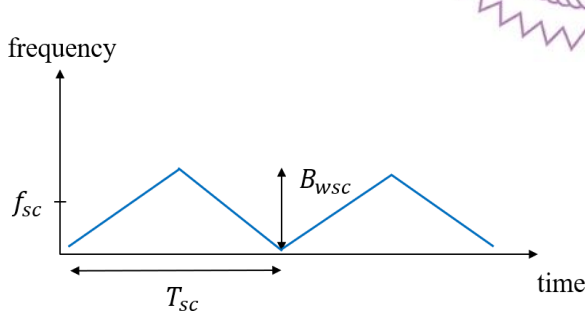


Figure 6. Slow chirp FMCW

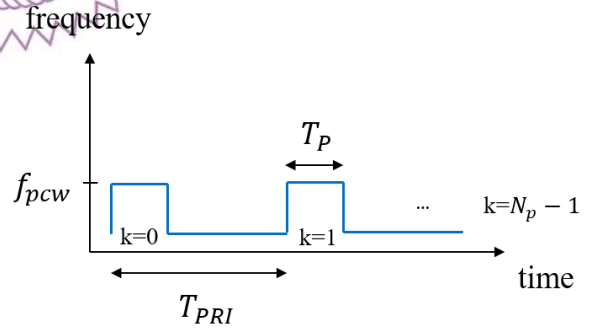


Figure 7. Pulsed CW

(d) Pulsed CW (a.k.a. Square-wave modulation): This modulation is used for a very precise distance measurement at close range by phase comparison of the two echo signal frequencies, shown in Figure 7. The transmitted signal is given by

$$s_{pcw}(t) = A_T \left(j2\pi \left(\sum_{k=0}^{N_p-1} f_{pcw} \Pi \left(\frac{t - kT_{PRI}}{T_p} \right) t \right) \right), 0 \leq t < T$$

Where f_{pcw} is the carrier frequency, Π is the square wave, the total number of pulse that we sent is N_p , T_{PRI} is the pulse repetition interval (PRI), and T_p is the period of the impulse.

(e) FSK (a.k.a. Stepped modulation): This is used for interferometric measurements and expands the unambiguous measuring range, shown in Figure 8. The transmitted signal is given by $s_{tfsk}(t) = A_T \exp \left(j2\pi \left(f_{fsk} - f_{step} \left(\frac{N_{step}-1-2(i \bmod N_{step})}{2} \right) \right) t \right)$, $0 \leq t < T$ where f_{fsk} is the carrier frequency, f_{step} is the difference frequency of adjacent steps, and N_{step} is the number of total steps.

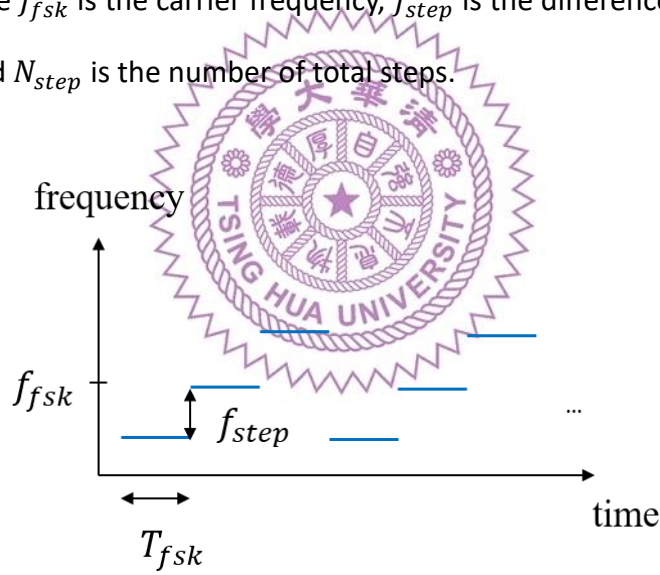


Figure 8. FSK modulation

2.1.4 Radar Object Detection Pipeline

As shown in Figure 9, the conventional radar detection pipeline consists of four steps: (a) CFAR detection, (b) clustering, (c) feature extraction, and (d) classification.

(a) CFAR detection: A CFAR detector is applied to detect peaks in the RD heat map as a list of targets. CFAR is usually executed in an on-chip DSP, so the choice of method is restricted by hardware support.

(b) Clustering: The moving targets are first projected to Cartesian coordinates and clustered by DBSCAN [7]. Static targets are usually filtered out before clustering because they are indistinguishable from environmental clutter. Clustering is the most important stage in the radar detection pipeline, especially for the next-generation high-resolution radar [8].

(c) Feature extraction: Within each cluster, hand-crafted features, such as the statistics of measurements and shape descriptors, are extracted.

(d) Classification: Then we can feed the processed data and the hand-crafted features to a ML classifier to do radar target classification. Researchers have found that range and Doppler features are most important for classification, while angle and shape features are usually discarded, probably because of the low angular resolution [9].

Chapter 3 Case Study – TI AWR 2944 EVM

3.1 TI AWR 2944 EVM Overview

The AWR2944 evaluation module (EVM) as shown in Figure 9 is an easy-to-use platform for evaluating the AWR2944 millimeter-wave system-on-chip (SoC) radar sensor, which has direct connectivity to the DCA1000EVM (sold separately).

The AWR2944EVM kit contains everything required to start developing software for the on-chip C66x digital signal processor (DSP), Arm Cortex-R5F controller, and hardware accelerator (HWA 2.0).

Also included is onboard emulation for programming and debugging, as well as onboard buttons and LEDs for quick integration of a simple user interface [10].

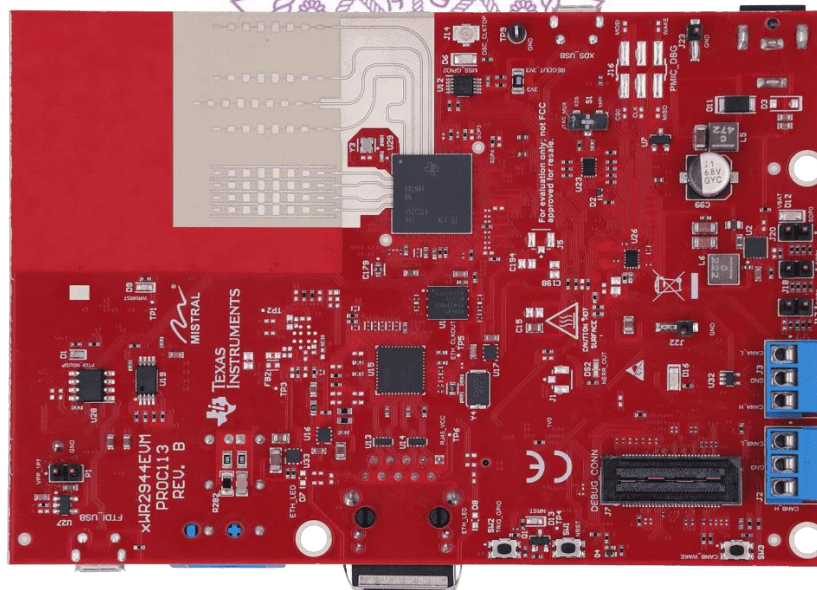


Figure 9. AWR2944EVM

3.2 TI AWR 2944 EVM Features

1. 76-GHz to 81-GHz millimeter-wave radar sensor.
2. Onboard four-transmit four-receive (4TX/4RX) antenna.
3. On-chip C66x DSP core and Arm Cortex-R5F controller.
4. On-chip hardware accelerator (HWA 2.0) for FFT calculations.
5. Direct interface with DCA1000EVM.

3.3 TI AWR 2944 Spec

The AWR2944 is a single chip millimeter-wave Sensor composed of a FMCW transceiver that operating in the 76-81 GHz band, radar data processing elements, and peripherals for in-vehicle networking. The parameters are shown in Table 3 [11].

3.3.1 TI AWR 2944 chip parameters

Number of receivers	4
Number of transmitters	3, 4
ADC sampling rate (Max) (MSPS)	37.5
Interface type	2 CAN-FD, Ethernet, I2C
DSP	C66x DSP 360MHz
Hardware accelerators	Radar hardware accelerator
Rating	Automotive
Operating temperature range (C)	-40 to 140
Power supply solution	LP87745-Q1
Security	Cryptographic acceleration, Device identity/keys, Secure boot, Secure software update, Software IP protection, Trusted execution environment

Table 3. TI AWR2944 parameters

3.3.2 Block Diagram

The block diagrams of TI AWR2944 chip are shown in Figure 10 and Figure 11 [11].

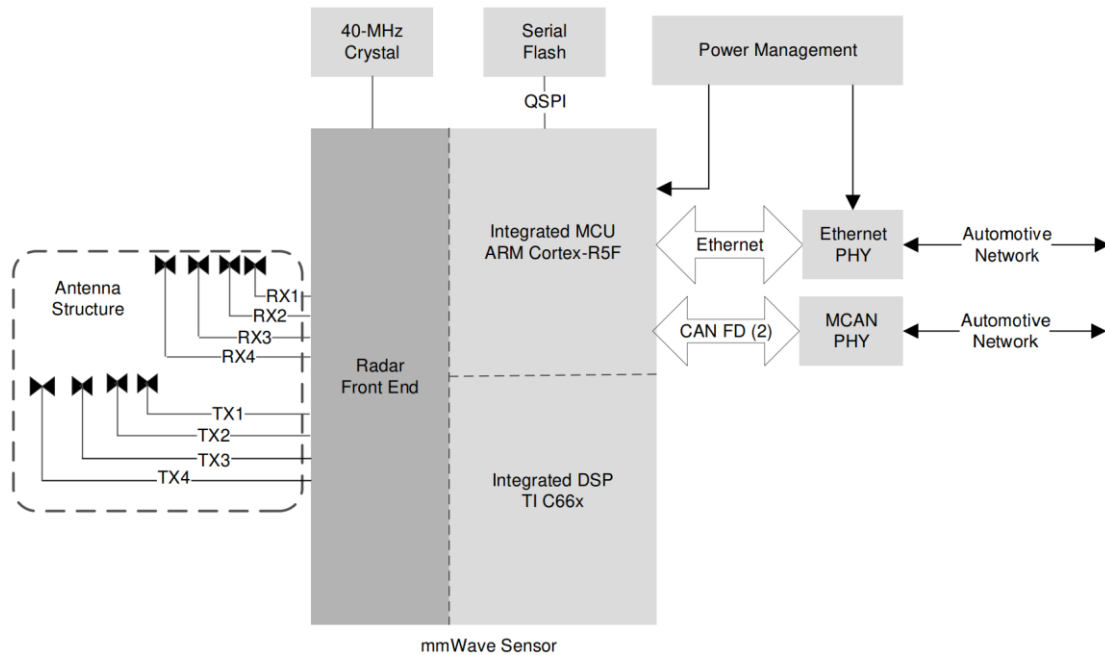


Figure 10. Functional Block Diagram

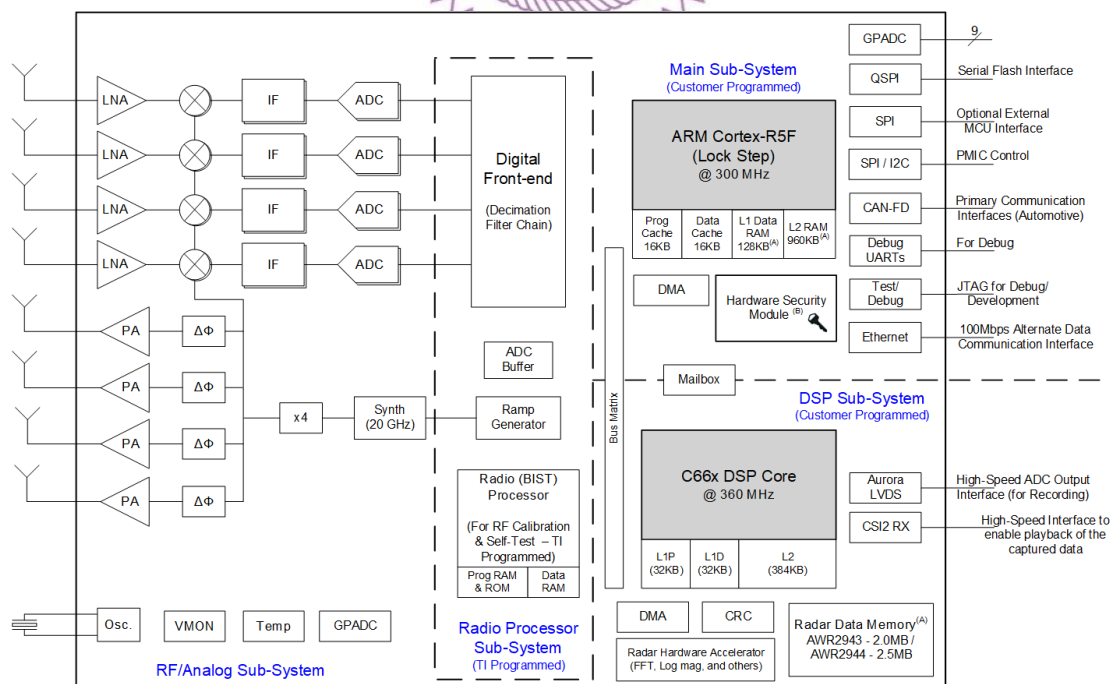


Figure 11. Block Diagram

Chapter 4 Applications and its opponents

4.1 Applications

Radar MCUs have been widely used in active safety functions such as automatic emergency braking (AEB) and forward collision warning (FCW), as mentioned previously in chapter 1. Radar perception algorithm has great potential in autonomous driving systems, and we are looking forward to seeing the use of radar sensors in Tesla's Autopilot system.

In addition to self-driving applications, radar sensors can also be used for non-contact vital sign detection. Vital signs, including the heart rate and breath rate, are the most fundamental and crucial indicators for clinical diagnosis. Conventional contact devices, e.g., electrocardiogram (ECG), photoplethysmography (PPG), and respiratory inductance plethysmography (RIP), are widely used to measure vital signs for healthcare applications. However, a close contact with electrodes and wires may cause skin discomfort and inconvenience, as well as viral infections. Therefore, measuring with a non-contact device is a better option. The target avoids electrodes that are in close contact on the body, which is most beneficial.

4.2 Opponents

In self-driving applications, radar has two strong competitors: vision and LiDAR.

4.2.1 Vision - Comma ai Driver Assistance System

The comma three is custom hardware designed to live in your car, and purpose built to run openpilot. The comma three has three beautiful HDR cameras, two cameras to watch the road and one night-vision camera to see inside the car.

Besides cameras, the comma three has a suite of connectivity and sensors including cellular LTE, Wi-Fi, an IMU, high-precision GPS, and microphones. The tech spec is shown in Table 4 [12].








	CAMERAS
Three 1080p cameras w/ 120 dB of dynamic range: dual-cam 360° vision and a narrow cam to see far-away objects	
	PROCESSOR
Qualcomm Snapdragon 845	
	STORAGE OPTIONS
<ul style="list-style-type: none"> - 32GB built in storage - Samsung 980 NVMe SSD (250GB or 1TB) 	
	CONNECTIVITY
<ul style="list-style-type: none"> - LTE - Wi-Fi - High-Precision GPS 	
	NIGHT-VISION
IR LEDs for interior night-vision monitoring	
	DISPLAY
2160×1080 Beautiful OLED display	
	PORTS
<ul style="list-style-type: none"> - OBD-C port (USB-C w/ CAN) - USB 3.1 Gen 2 port (DisplayPort capability) 	

Table 4. Comma Three spec

4.2.2 LiDAR - Velodyne HDL-64E LiDAR Sensor

LiDAR is divided into mechanical LiDAR, semi-solid LiDAR, and pure solid-state LiDAR. These three types of LiDARs have their advantages and disadvantages. Due to good reliability, lower cost, and relatively mature technology, semi-solid LiDARs have become the mainstream in the current market.

However, in contrast, pure solid-state LiDAR has faster scanning speed, higher accuracy, better controllability, and smaller size. It is generally regarded by the industry as the technical direction of the long-term development of LiDAR, but the technology is not fully mature at present. The design of pure solid-state LiDAR with no moving parts will achieve higher reliability and integration, but the current technology is immature and faces problems such as short-ranging and low resolution. Under the industry trend of pursuing solid-state LiDAR, laser energy density and laser modulation will be a major technical bottleneck.

In addition, many industry insiders ascribed the development bottleneck of LiDAR to price. At present, the mechanical LiDAR price is generally high, and it is mainly used in test vehicles. For instance, the price of Velodyne's 64-line LiDAR is \$80,000, its shown in Figure 12 and its spec is shown in Table 5. There are several different technical routes for LiDAR, their working principles are different, and they currently are in bloom. It is expected that the LiDAR price will drop significantly within 3 to 5 years, which is an important prerequisite for its large-scale application [13].



Figure 12. Velodyne's 64-line LiDAR

■ Sensor

- Time of Flight Distance Measurement with Intensity
- 64 channels
- Measurement Range: Up to 120 m
- Single or Dual Returns
- Field of View (Vertical): $+2.0^{\circ}$ to -24.9° (26.9°)
- Angular Resolution (Vertical): 0.4°
- Field of View (Horizontal): 360°
- Angular Resolution (Horizontal/Azimuth): $0.08^{\circ} - 0.35^{\circ}$
- Rotation Rate: 5 Hz – 20 Hz

■ Laser

- Laser Product Classification: Class 1 Eye-safe
- Wavelength: 903 nm
- Dynamic Laser Power Selection for Larger Dynamic Range

Table 5. Velodyne's 64-line LiDAR spec

Chapter 5 Conclusion

Finally, we conclude with the SWOT analysis shown in Table 6.

■ SWOT

■ Strengths

- Long detection range
- All-weather operation
- Low power consumption
- Low cost

■ Weaknesses

- Low angular resolution
- Hard to detect stationary object

■ Opportunities

- Autonomous driving
- Vital sign detection

■ Threats

- Vision
- LiDAR

Table 6. SWOT analysis of Radar Sensors

Reference

- [1] Zhou, Yi, et al. "Towards Deep Radar Perception for Autonomous Driving: Datasets, Methods, and Challenges." *Sensors* 22.11 (2022): 4208.
- [2] Karpathy, A. Keynotes at CVPR Workshop on Autonomous Driving. 2021. Available online: <https://cvpr2021.wad.vision/> (accessed on 31 December 2022).
- [3] Fred Lambert. "Tesla says it is adding radar in its cars next month amid self-driving suite concerns" Available online: <https://electrek.co/2022/12/06/tesla-radar-car-next-month-self-driving-suite-concerns/> (accessed on 31 December 2022).
- [4] G. Hakobyan and B. Yang, "High-Performance Automotive Radar: A Review of Signal Processing Algorithms and Modulation Schemes," in *IEEE Signal Processing Magazine*, vol. 36, no. 5, pp. 32-44, Sept. 2019.
- [5] Ramasubramanian, Karthik, and T. Instruments. "Using a complex-baseband architecture in FMCW radar systems." *Texas Instruments* 19 (2017).
- [6] Kim, Jinwook, Seongwook Lee, and Seong-Cheol Kim. "Modulation type classification of interference signals in automotive radar systems." *IET Radar, Sonar & Navigation* 13.6 (2019): 944-952.
- [7] Schubert, Erich, et al. "DBSCAN revisited, revisited: why and how you should (still) use DBSCAN." *ACM Transactions on Database Systems (TODS)* 42.3 (2017): 1-21.
- [8] Scheiner, Nicolas, et al. "Off-the-shelf sensor vs. experimental radar-How much resolution is necessary in automotive radar classification?." *2020 IEEE 23rd International Conference on Information Fusion (FUSION)*. IEEE, 2020.
- [9] N. Scheiner, N. Appenrodt, J. Dickmann and B. Sick, "Radar-based Road User Classification and Novelty Detection with Recurrent Neural Network Ensembles," *2019 IEEE Intelligent Vehicles Symposium (IV)*, 2019, pp. 722-729.

- [10] TI AWR 2944 EVM. Available online: <https://www.ti.com/tool/AWR2944EVM> (accessed on 31 December 2022).
- [11] TI AWR 2944 Spec. Available online: <https://www.ti.com/product/AWR2944> (accessed on 31 December 2022).
- [12] Comma-three Spec. Available online: <https://comma.ai/shop/comma-three> (accessed on 31 December 2022).
- [13] Neuvision, Inc. “Velodyne 64-line LiDAR” Available online: <https://www.neuvision.com/media/blog/lidar-price.html> (accessed on 31 December 2022).

